LEGIBILITY NOTICE

A major purpose of the Technical Information Center is to provide the broadest dissemination possible of information contained in DOE's Research and Development Reports to business, industry, the academic community, and federal, state and local governments.

Although a small portion of this report is not reproducible, it is being made available to expedite the availability of information on the research discussed herein.

LA-UR -87-3488

LA-UR--87-3488

DE88 003184

Los Alamos National Laboratory is operated by the University of California for the United States Department of Energy under contract W-7405-ENG-36

TITLE: DIRECT MASS MEASUREMENTS OF LIGHT NEUTRON-RICH NUCLEI USING FAST RECOIL SPECTROMETERS

AUTHOR(S): D. J. Vieira
J. M. Wouters

SUBMITTED TO: Nuclei Far From Stability
Rosseau Lake, Ontario, Canada
Sept. 14-19, 1987

MASTER

Los Alamos

Los Alamos National Laboratory
Los Alamos, New Mexico 87545

DIRECT MASS MEASUREMENTS OF LIGHT NEUTRON–RICH NUCLEI USING FAST RECOIL SPECTROMETERS

David J. Vieira, Jan M. Wouters, and the TOFI Collaboration
Los Alamos National Laboratory, Los Alamos, NM 87545

ABSTRACT

Extensive new mass measurement capabilities have evolved with the development of recoil spectrometers. In the Z=3–9 neutron–rich region alone, 12 neutron–rich nuclei have been determined for the first time by the fast–recoil direct mass measurement method. A recent experiment using the TOFI spectrometer illustrates this technique. A systematic investigation of nuclei that lie along or near the neutron–drip line has provided a valuable first glimpse into the nuclear structure of such nuclei. No evidence for a large single–particle energy gap at N=14 is observed; however, a change in the two–neutron separation energy trend is found at N=15. This change is correctly predicted by shell model calculations, and is interpreted in terms of the smaller $1s_{1/2}$–$1s_{1/2}$ interaction compared to that of the $0d_{5/2}$–$0d_{5/2}$ neutron–neutron interaction.

INTRODUCTION

In the study of light exotic nuclei, the ground state mass is often one of the first pieces of quantitative information to be learned about a "new" or previously unobserved nucleus. Because the mass of a nucleus reflects the interplay of nuclear and Coulomb forces, valuable insight into the nuclear structure of such nuclei can be obtained from their measurement. In the present case, we seek to test and refine our understanding of nuclei that lie far from the valley of β–stability. Do these exotic nuclei have the same type of shell structure as nuclei that lie close to stability? Can the new regions of deformation being observed in exotic nuclei be understood in terms of conventional models? And does the nucleon–nucleon pairing energy decrease with increasing isospin, as recently suggested by Vogel *et al.*?[1] We can take the first steps toward answering these and other interesting questions by making a systematic investigation of the masses of exotic nuclei.

In this paper, we concentrate on the masses of light neutron–rich nuclei. The current status of the mass surface in this region is shown in Fig. 1, where the shading of each square shows the accuracy with which the mass of each isotope has been measured. Since the compilation of Wapstra and Audi,[2] several new measurements have been performed (indicated by the darker shaded squares in Fig. 1). Of the 27 isotopes whose masses have been determined for the first time, 21 were measured with fast recoil spectrometers. This new technique relies on the direct mass measurement of fast reaction products. The method is not only fast (transit time ~1 μsec) and accurate (σ_m/m = 10–100 ppm; σ_m= 100–1000 keV, depending on production rates), but it also permits the simultaneous mass determination of many nuclei throughout an entire A and Z region. The first examples of such measurements have been carried out in the light mass region; these examples are highlighted in this and the following paper.[3]

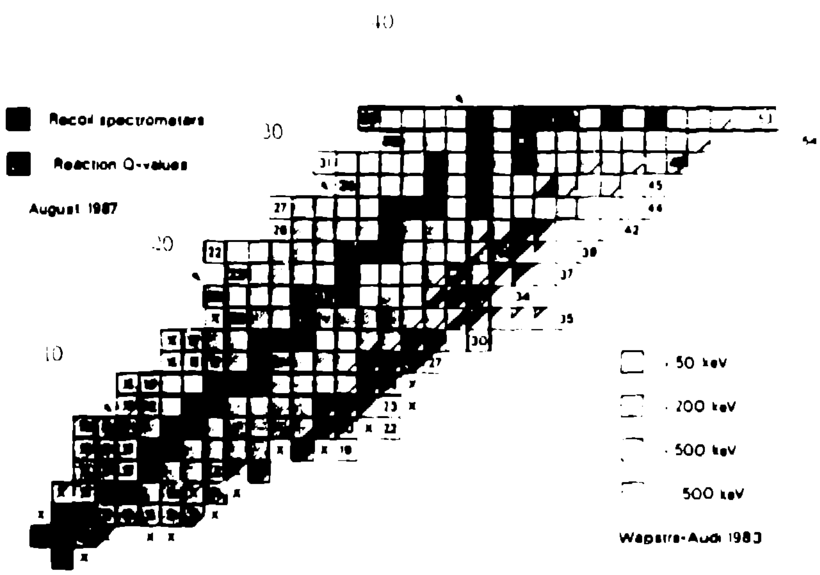

FIG. 1. A section of the chart of the nuclides showing the light mass region. Stable nuclei are indicated by black squares; nuclei whose masses have been determined are shaded according to their quoted accuracy (see Ref. 2); open squares indicate nuclei which have been identified to be stable with respect to prompt nucleon (two-nucleon) emission, but for which no mass has been reported; and X indicates nuclei that are nucleon unstable. Recent mass measurements are indicated by darker shaded squares (see legend).

The recoil spectrometer developments have been pioneered by two groups, one working with the energy-loss spectrometer (SPEG) at the Grand Accélérateur National d'Ions Lourds (GANIL) and the other using the Time-of-Flight Isochronous (TOFI) spectrometer at the Los Alamos Meson Physics Facility (LAMPF). At GANIL, projectile fragmentation reactions are used to produce exotic nuclei, and a combined velocity and magnetic rigidity measurement is employed to produce mass determinations. In contrast, LAMPF uses proton-induced target fragmentation reactions as a source of neutron-rich nuclei and employs a new type of time-of-flight recoil spectrometer to extract masses from a high-resolution, mass-to-charge determination. Both groups have made extensive measurements throughout the light-mass neutron-rich region. We will restrict our discussion to the Z=3–9 neutron-rich region, whereas the following paper will concentrate on the Z=10–15 region.

TOFI MEASUREMENTS IN THE Z=3–9 REGION

To illustrate these measurements, we will briefly describe a recent experiment using the TOFI spectrometer (see Ref. 4 for more details).

A schematic of the TOFI spectrometer and its associated transport line is shown in Fig. 2. Large yields of exotic nuclei are produced in the scattering chamber when LAMPF's 1-mA, 800-MeV proton beam strikes a 1-mg/cm^2

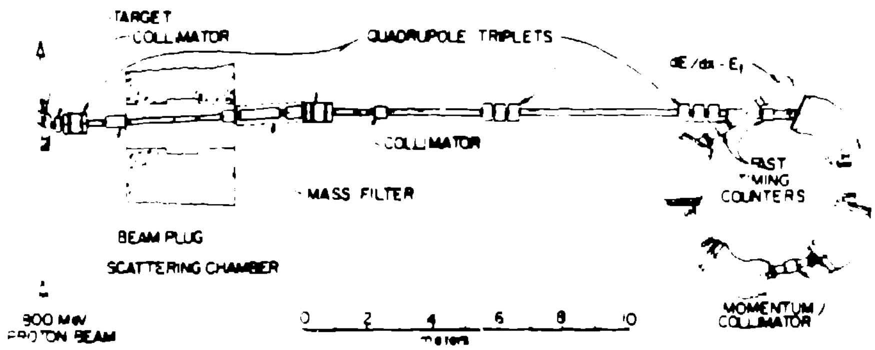

FIG. 2. Schematic of the TOFI spectrometer and its associated transport line.

^{nat}Th target. Some of the reaction products recoiling out of the target are captured by a secondary beam transport line.[5] Because proton–induced target fragmentation is not strongly angle dependent at this energy, the transport line has been conveniently located at ~90 degrees to the primary beam.

The transport line consists of four electromagnetic quadrupole triplets and a small, separated–sector mass–to–charge filter. A collimator is located at the intermediate focus position (approximate halfway through the line), where a mass–to–charge dispersed image of the illuminated target spot is produced. Here the high rate of uninteresting ions with mass–to–charge ratios (M/Q) of < 2.0 are greatly reduced to avoid count rate problems in the spectrometer. In the second half of the transport line, the velocities of the recoils are measured over a path length of ~10 m by thin–foil, secondary–electron, microchannel-plate (MCP) intensified, fast–timing detectors[6] located both just downstream from the M/Q collimator and at the entrance of the spectrometer.

The spectrometer has been designed to be isochronous so that the flight time of ions passing through the system provides a precise measure of the mass–to–charge ratio.[7] Four identical dipole magnets are arranged so that ions of a particular mass–to–charge ratio, but of lower (or higher) velocity than the selected mean velocity, take a shorter (or longer) path length through the system in such a way that the same overall flight time results. In addition, the spectrometer is one–to–one imaging and nondispersive overall so that small-area, fast–timing detectors can be used while a reasonably large solid angle and momentum–to–charge acceptance ($\Omega = 2.5$ msr and $\delta(p/Q)/(p/Q) = 4\%$) are maintained. The fourfold unit–cell symmetry of the system leads to small timing aberrations that result in high mass–to–charge resolution for a wide range of M/Q species without using ray–tracing techniques. In this experiment where the spectrometer was set for a momentum–to–charge of 210 MeV/c/Q, a timing resolution of ~180 ps (FWHM) was obtained between two MCP fast–timing detectors (one located at the entrance and the other at the exit of the spectrometer). For a typical flight time of ~500 ns, a relative time resolution—and consequently mass–to–charge resolution—of $\delta T/T = \delta(M/Q)/(M/Q) = 3.6 \times 10^{-4}$ was obtained. This performance was limited by the fast–timing detectors and their associated electronics and *not* by the intrinsic resolution of the spectrometer.

Masses are extracted from the measured mass–to–charge (time–of–flight) spectra that have been gated according to atomic number and charge state (see Fig. 3). The atomic number was determined from measurements of the ion's velocity and stopping power; the charge state was obtained from the measured velocity, total energy, and mass–to–charge ratio. In the present experiment, the stopping power and total energy were measured in a ΔE (20–μm) – E (720–μm) silicon detector telescope positioned immediately downstream from the MCP detector at the exit of TOFI. To further reduce the effects of isobaric cross–contamination, the mass resolution of TOFI was used to directly resolve isobars.

Using the direct mass measurement approach, the centroid of each M/Q line (determined by moments analysis) is related to the mass of that particular species. The centroids of lines with known masses were used to calibrate the system so that the masses of "unknown" lines could be determined. Small corrections to each centroid were made to account for time–to–amplitude walk and nonlinearities of the electronics. A typical calibration contained ~80 known

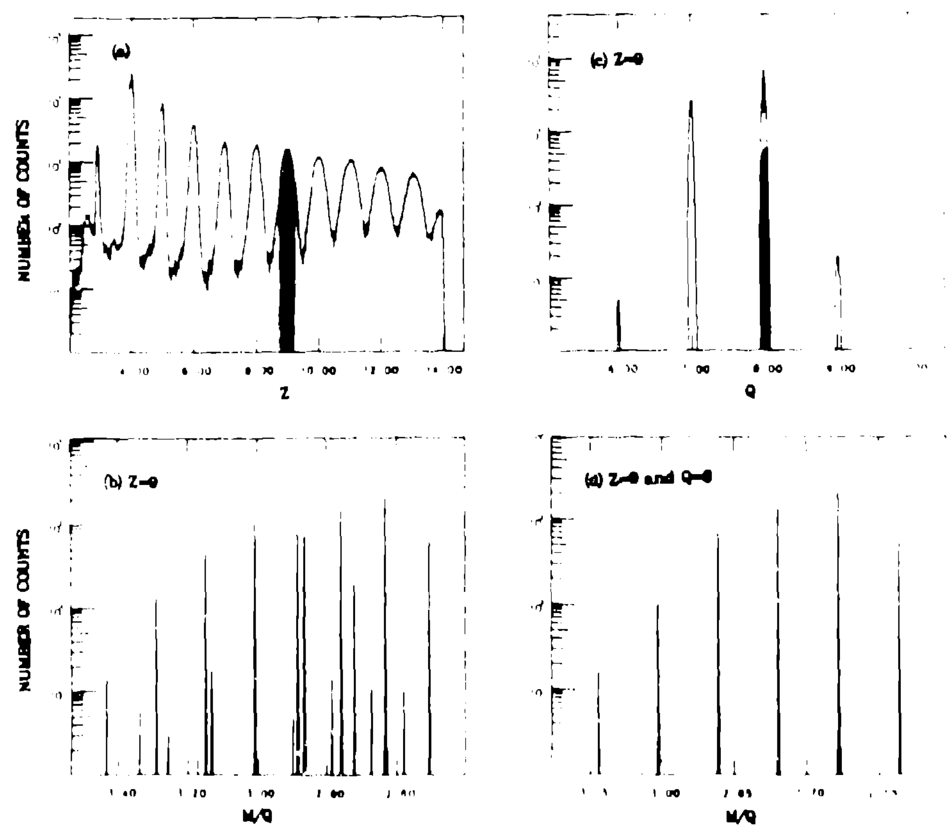

FIG. 3. (a) An ungated Z spectrum collected in a 24–h period; (b) and (c) the corresponding M/Q and Q spectra obtained for Z=9 selected events; (d) the resulting Z=9 and Q=8 gated M/Q spectrum. The measured Z, Q, and M/Q resolutions are 3.5%, 1%, and 3.6×10^{-4} (FWHM), respectively.

mass-to-charge lines. Table I shows final masses determined from a weighted average measurement of several runs (and different charge states where possible) taken over a 4-week data collection period. The quoted uncertainties result from a sum of statistical, calibration, and systematic uncertainties; the latter equaled ~2% of the line (~17 keV/Q).

DISCUSSION

Figure 4 shows a comparison of all recent mass measurements in the Z=3-9 neutron-rich region. There is excellent agreement in all cases except ^{14}Be and ^{22}N, were the measurements disagree at slightly beyond the one standard deviation level. Refinements in the fast-recoil direct mass measurement technique are indicated by both the reductions in errors and the determination of additional neutron-rich nuclei with each successive experiment. Of the nuclei that have been shown to be stable with respect to prompt neutron (or two-neutron) emission,[12] only the masses of ^{19}B, ^{22}C, and ^{23}N remain to be measured.

In Fig. 5, the masses are plotted in terms of the two-neutron separation energy, S_{2n}, *vs* neutron number. This plot provides a convenient way of removing odd-even neutron-pairing energy effects so that other nuclear structure features, such as energy gaps in the single-particle levels or changes in nuclear deformation, stand out more clearly. Of particular interest here is the question of a subshell closure at N=14. If a large energy gap between the neutron $0d_{5/2}$ and $1s_{1/2}$ energy levels did exist, a significant decrease in S_{2n} values after N=14 would be expected. However, for the neutron-rich isotopes of oxygen, fluorine,

TABLE I. Total number of observed events and determined mass excesses (errors given in parentheses).

^{A}Z	No. of Events	Mass Excess (μu)[a]	Mass Excess (MeV)
^{11}Li	168	43780 (130)	40.78 (.12)
^{14}Be	95	42600 (150)	39.74 (.14)
^{17}B	106	46830 (180)	43.62 (.17)
^{19}C	700	35180 (130)	32.77 (.12)
^{20}C	82	40360 (240)	37.60 (.22)
^{20}N	13,015	23380 (130)	21.78 (.12)
^{21}N	2,733	26930 (210)	25.09 (.20)
^{22}N	110	34340 (250)	31.99 (.23)
^{23}O	949	15700 (150)	14.62 (.14)
^{24}O	61	20000 (500)	18.6 (.5)
^{25}F	3,312	12210 (150)	11.37 (.14)
^{26}F	363	19820 (210)	18.46 (.20)
^{27}F	15	27500 (700)	25.6 (.7)

[a] Although nuclei with long-lived ($\tau > 150$ ns) isomeric states are rare in this region, the population of an, as yet unknown, isomeric state in one of these isotopes cannot be excluded on the basis of this data.

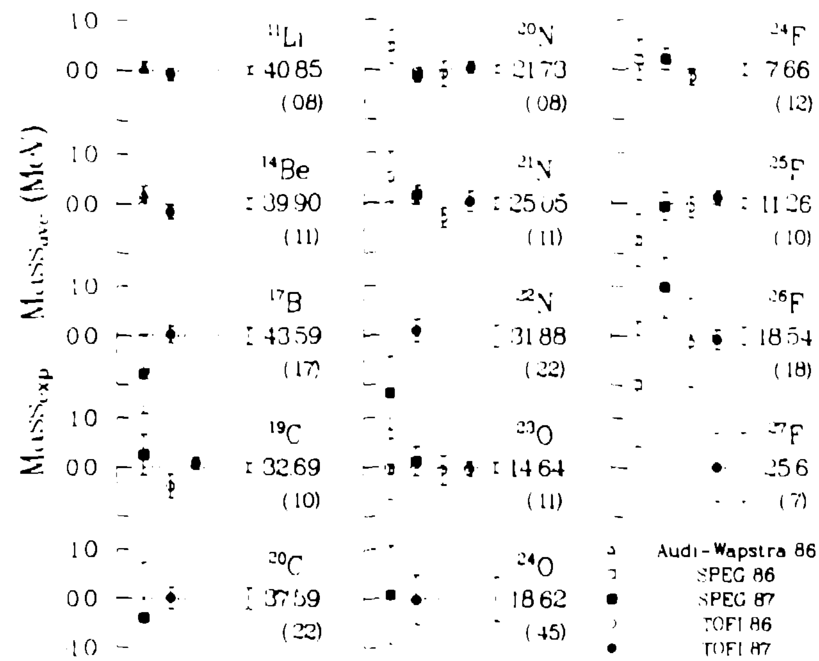

FIG. 4. A comparison of recent mass measurements for Z=3–9 neutron-rich nuclei. The weighted average mass excess is given in MeV for each isotope; errors are given in parentheses. The legend references are: Audi–Wapstra 86 – Ref. 8; SPEG 86 – Ref. 9; SPEG 87 – Ref. 10; TOFI 86 – Ref. 11; and TOFI 87 – Ref. 4 and this work.

and neon, no change in the S_{2n} trend is found at N=14, but rather at N=15! What is happening in this region?

As noted in Ref. 11, the spherical shell model calculations of Wildenthal *et al.*[13] reproduce the S_{2n} values throughout the sd shell region very well, with the notable exception of the deformed N=20 region. Based on the good agreement found in the N=14–16 region (see Fig. 6) and by the fact that the ground state wave functions are calculated to be relatively pure a simple shell model interpretation of the observed S_{2n} trend can be advanced. First, we point to the fact that no large decrease in S_{2n} values is observed in going from N=14 to N=15. This indicates that no large energy gap exists between the $0d_{5/2}$ and $1s_{1/2}$ neutron levels. (In Ref 13, ~1-MeV energy gap between these levels is given, which is a typical ground state level spacing in these light nuclei.) Second, the more rapid decrease in S_{2n} values between N=15 and N=16 can be explained by the difference in the $0d_{5/2}$–$0d_{5/2}$ and the $1s_{1/2}$–$1s_{1/2}$ neutron–neutron interaction energies (the former is calculated to be nearly twice as large as that of the latter), for it is not until N=16 that no $d_{5/2}$–$d_{5/2}$ interaction is involved in the removal of two–neutrons. This provides a qualitative interpretation of the change in the S_{2n} trend observed at N=15.

When these mass measurements are compared to the psd shell model calculations of Brown *et al.*[14] (see Fig. 6), good agreement is found for the carbon and nitrogen isotopes, but increasing deviations are noted as one moves to lighter nuclei. The theoretical under-estimation of binding found for ^{26,27}F

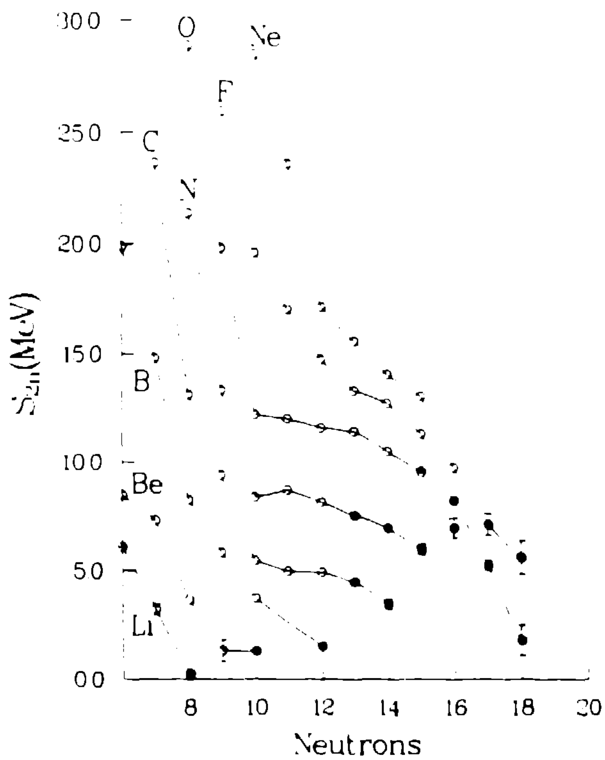

FIG. 5. Two–neutron separation energy *vs* neutron number for isotopes of lithium to neon. Solid circles indicate nuclei that have been measured by fast recoil spectrometers, and the open circles show data taken from Ref. 8. Error bars are indicated where they are larger than the symbol size.

could be related to the onset of prolate deformation, as observed for the N=19–20 isotones of sodium and magnesium, but the measurements of ^{29,30}Ne are needed to confirm this interpretation.

In Fig. 7, comparisons to three other approaches are seen. The macroscopic–microscopic model of Tachibana *et al.*[15] gives reliable masses, except in the N=15–17 region. This likely reflects a deficiency in the microscopic part of the calculation because for nuclei that lie close to stability (e.g., ^{28}Si), a rapid decrease in binding occurs after N=14; we do not observe this feature in the case of these neutron–rich nuclei. Thus, calculations that rely on the masses of nuclei lying close to stability would be expected to underestimate the binding energy of these exotic nuclei. Similar trends are also noted for the macroscopic–microscopic models of Möller and Nix[16] and Möller *et al.*[17] (not shown in Fig. 7) and, to a much smaller extent, for the latest Garvey–Kelson mass relationship predictions of Jänecke and Masson[18] and the updated modified shell model calculations of Wouters *et al.*[4] Finally, a significant overestimation of binding is evident for the Garvey–Kelson predictions for ^{20}C and ^{21,22}N. This can be explained in a manner analogous to the arguments above, but in this case the nuclei used by the mass relationship are at or near the deformed ^{20}Ne region. The increased binding afforded by this deformation then leads to a more bound

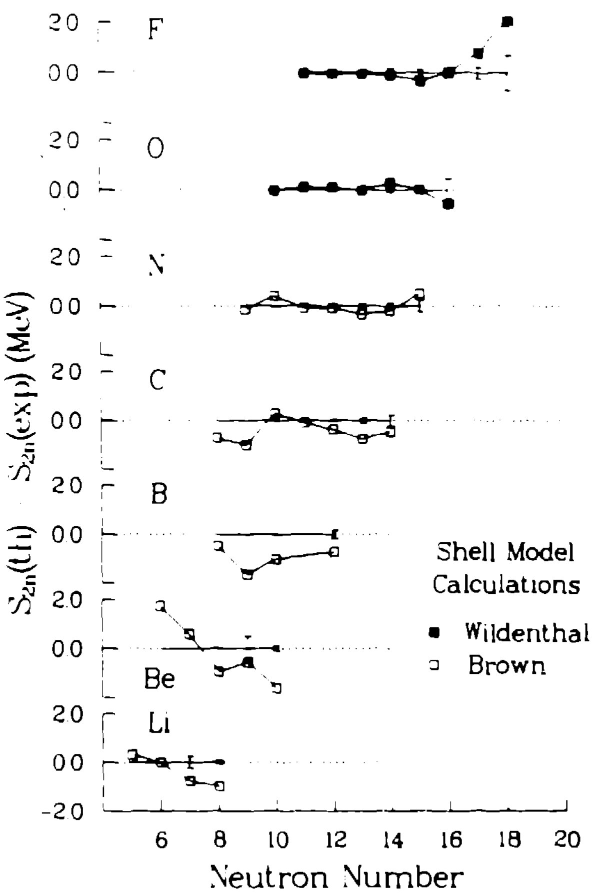

FIG. 6. Two–neutron separation energy difference between shell model predictions and those experimentally determined *vs* neutron number. The solid squares indicate calculations of Ref. 13 and the open squares indicate Ref. 14. Error bars represent the experimental uncertainties.

mass prediction for N=14, 15 isotones of carbon and nitrogen, which are expected to be spherical in shape.

CONCLUSION AND OUTLOOK

In summary, the development of fast recoil spectrometers has significantly advanced our mass measurement capabilities for exotic light nuclei. Some 12 isotopes have been determined for the first time in the Z=3–9 neutron-rich region alone. This progress has lead to an improved understanding of the light mass surface. There is no evidence for a subshell closure at N=14 in these measurements; however, the indication of a weaker $s_{1/2}$–$s_{1/2}$ interaction compared to that of the $d_{5/2}$–$d_{5/2}$ neutron–neutron interaction is evident in

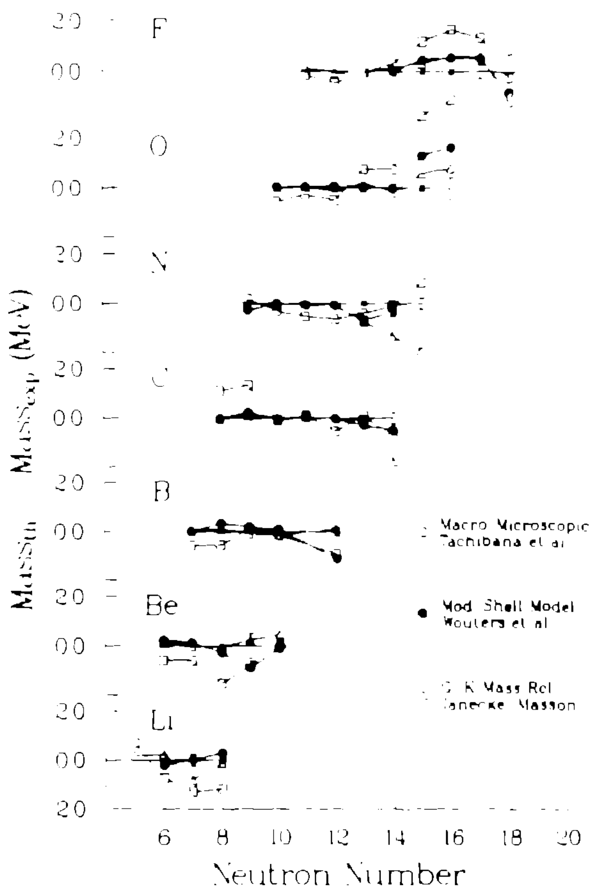

FIG. 7. Mass difference between theoretical predictions of Ref. 15 (open squares), Ref. 4 (solid circles), and Ref. 16 (open triangles), and the measured experimental results *vs* neutron number, as in Fig. 6.

S_{2n} trend and is supported by shell model calculations. In the future, further progress can be expected as fast recoil spectrometers are applied to the mass measurement of heavier nuclei.

ACKNOWLEDGMENTS

We wish to acknowledge G. T. Garvey, P. Möller, J. R. Nix, and B. H. Wildenthal for valuable discussions and comments concerning this work. We thank B. A. Brown for providing us with his shell model calculations before publication. Special thanks are extended to C. E. Lowe, J. H. Heiken, and G. L. Tietjen for help in preparing this manuscript. The following members of the TOFI collaboration have also made significant contributions to this work and are gratefully acknowledged: G. W. Butler, (Los Alamos National Laboratory); K. Vasiri and V. G. Lind (Utah State University); R. H. Kraus, Jr. and

D. S. Brenner (Clark University); F. H. Wohn (Iowa State University); K. E. G. Lõbner (University of Munich); A. H. Wapstra (Nuclear Institute for Nuclear and High-Energy Physics, Amsterdam). This work was performed under the auspices of the U.S. Department of Energy.

REFERENCES

1. P. Vogel, B. Jonson, and P. G. Hansen, Phys. Lett. **139B**, 227 (1984).
2. A. H. Wapstra and G. Audi, Nucl. Phys. **A432**, 1 (1985).
3. W. Mittig, *et al.*, these proceedings.
4. J. M. Wouters, *et al.*, to be published.
5. K. Vaziri, *et al.*, Nucl. Instr. Meth. **B26**, 280 (1987).
6. R. H. Kraus, Jr., *et al.*, Nucl. Instr. Meth. A (in press).
7. J. M. Wouters, *et al.*, Nucl. Instr. Meth. **A240**, 77 (1985); J. M. Wouters, *et al.*, Nucl. Instr. Meth. **B26**, 286 (1987).
8. G. Audi and A. H. Wapstra, Interim Mass Adjustment, April 1986, At. Data Nucl. Data Tables (in press).
9. A. Gillibert, *et al.*, Phys. Lett. **B176**, 317 (1986).
10. A. Gillibert, *et al.*, Phys. Lett. **B192**, 39 (1987).
11. D. J. Vieira, *et al.*, Phys. Rev. Lett. **57**, 3253 (1986).
12. F. Pougheon, *et al.*, Europhys. Lett. **2**, 505 (1986).
13. B. H. Wildenthal, Prog. Part. Nucl. Phys. **11**, 5 (1984); B. H. Wildenthal, M. S. Curtin, and B. A. Brown, Phys. Rev. C **28**, 1343 (1983).
14. B. A. Brown, private communication; M. S. Curtin, *et al.*, Phys. Rev. Lett. **56**, 34 (1986).
15. Tachibana, *et al.* At. Data Nucl. Data Tables (in press); and these proceedings.
16. P. Möller and J. R. Nix, At. Data Nucl. Data Tables (in press).
17. P. Möller, *et al.*, *ibid.*
18. J. Jänecke and P. J. Masson, *ibid.*